ELSEVIER

Palaeogeography, Palaeoclimatology, Palaeoecology 129 (1997) 251–267

PALAEO

# A new approach to paleoclimatic research using linear programming

M.J. Kuby *, R.S. Cerveny, R.I. Dorn

*Department of Geography, Arizona State University, Tempe, AZ 85287-0104, USA*

Received 4 July 1996; revision 10 September 1996; accepted 10 September 1996

**Abstract**

One of the most frequently attempted correlations in Quaternary research is between insolation and paleoclimatic data. Yet there are a large number of insolation time series that could potentially explain a Quaternary dataset, individually or in combination. We computed 342 insolation time series (varying by latitude, time of year and time of day) for fitting to four different paleoclimatic records: foraminiferal $\delta^{18}O$ from SPECMAP; temperatures inferred from Vostok, Antarctica ice cores; marine accumulation rates of a freshwater diatom, *Melosira*, originating from tropical Africa lakebeds; and $\delta^{18}O$ variations in calcite at Devil's Hole, Nevada. We developed two "inductive" linear programming models that solve for the weighted combination of insolation curves that minimize either the average or maximum residual from the proxy curve. Each of the four proxy records, lagged and unlagged, was solved by both model types. On average, our composite insolation curves fit the proxy records 48–76% better than does June daily insolation at 60°N, the key insolation curve of the Milankovitch paradigm. Globally, high latitude insolation (60°–70° N and S) and insolation at specific times of day (noon or non-noon, as opposed to daily) dominated the results. Regionally, the model tended to select insolation curves from absolute latitudes similar to those of the proxy records. The fact that these results are plausible given known biophysical processes, combined with the fact that a small number of curves repeatedly accounted for a disproportionate share of the explanation, suggest strongly that the correlations found are not happenstance, despite the inductive method used.

*Keywords:* linear programming; Quaternary; Milankovitch; reconstruction; climate change; orbital parameters

## 1. Introduction

Many Quaternary researchers use deductive reasoning to link specific climatic processes to proxy records. In a landmark paleoclimatic study, however, Hays et al. (1976) used an inductive time-series approach to identify and isolate astronomical cycles in ocean sediment proxy records. Their analysis, combined with detailed reevaluation of Milankovitch's calculations of the Earth's not-perfectly-elliptical orbit (Berger, 1978), led to widespread acceptance of the astronomical theory of climate change. In this paradigm, insolation received at various latitudes fluctuates over tens of thousands of years, and summer solar radiation received at 60°N is thought to drive ice age fluctuations (Hays et al., 1976; Imbrie and Imbrie, 1980; Imbrie et al., 1992, 1993a).

This paper presents a different inductive approach based on linear programming (LP)

* Corresponding author.


*PII* S0031-0182(96)00118-6

(Dantzig, 1951), a mathematical optimization technique commonly used in engineering and business (e.g., Thomas and DaCosta, 1979; Shannon et al., 1980). We use LP to investigate linkages between insolation variability and paleoclimatic fluctuations.

There is precedent in the climatic change literature for using optimization procedures for fitting empirical climate reconstruction records to computed solar radiation records. Brüggemann (1992) uses a constrained optimization method, similar to LP in that a penalty cost function of deviations is minimized over the sum of a set of discrete time periods. Brüggemann's approach differs in that he accepts as a given the timing and content of the forcing radiation data, and he optimally tunes the timing of the age–depth relationship for sedimentation. We, on the other hand, accept the timing and measurement of the proxy records and radiation curves as given. However, instead of presuming that insolation at 60°N is the only control, as Brüggemann and other researchers (Martinson et al., 1987) do in the orbital tuning literature, we optimally choose the composite *set* of radiation forcing data.

Consequently, this paper is designed to serve two distinct purposes:

(1) We investigate LP's potential to provide new insights into Quaternary studies involving systems where the observed state of a response variable at any given place and time could have been produced by different combinations of a large number of predictor variables. In many such studies, it is preferable not to reduce the number of predictor variables, and yet traditional curve-fitting methods like Ordinary Least Squares (OLS) regression cannot handle very large numbers of combinations (Anderson et al., 1991).

(2) We apply LP to one of the most frequently attempted correlations in Quaternary research, between a paleoclimatic proxy record(s) and Milankovitch astronomical forcing mechanisms (precession, obliquity and eccentricity). We use LP to analyze the relative importance of long-term variations in solar radiation received at different latitudes, times of day (sun angles), and seasons in accounting for the variations in four major paleoclimatic proxy records. Such analyses, while not explanatory in themselves, can either lead or follow deduction.

Linear programming has a long tradition of use in natural sciences affiliated with Quaternary research, including ocean sediment chemistry (Leinen and Pisias, 1984), igneous petrology (Anderson et al., 1991), hydrology (Kachroo, 1992), natural resources (Dykstra, 1984) and geoarchaeology (Keene, 1981). However, LP has seen only limited use in Quaternary research.

## 2. Data

### 2.1. Paleoclimatic proxy records

We selected four well-known paleoclimate proxy records with different characteristics, thus providing an opportunity to assess LP as a screening tool:

(a) The 186,000 yr temperature signal from the "Vostok" Antarctic ice core is thought to reflect global climatic trends, but it may also be sensitive to insolation fluctuations in the higher latitudes of the Southern Hemisphere (Jouzel et al., 1987). Thus, the Vostok record offers an "intuitive test" of the LP method of insolation curve selection.

(b) The "SPECMAP" $\delta^{18}O$ record (Martinson et al., 1987) is a widely used indicator of global ice volume fluctuations. A potential complication is that SPECMAP is already "orbitally tuned" to 60°N Daily Insolation at June Solstice. This record is not, however, tuned to the other 341 insolation time series used. Computationally we were limited to the last 250,000 yr of the SPECMAP record.

(c) The desiccation of lakes in tropical Africa is represented by deep-sea sediment accumulation rates of the freshwater diatom *Melosira*. When lakes dry out, deflated diatoms are transported to the equatorial Atlantic (Pokras and Mix, 1987). This 250,000 yr record offers two challenging tests of the LP method. First, because the *Melosira* record is a tropical dataset, it should be influenced by tropical radiation (Pokras and Mix, 1987). Second, the *Melosira* record is marked by short-lived spikes which represent the onset of deflation, but not necessarily the full length of the arid period.

(d) The $\delta^{18}O$ record from the Devil's Hole,

Nevada, calcite core (DH-11) (Winograd et al., 1992), from 59,000 yr–250,000 yr, is the best-dated (Ludwig et al., 1992) terrestrial record of late-Pleistocene climatic change. The other three records do not have independent U-series age control. This record has been used to argue against the Milankovitch paradigm because the climatic signal precedes insolation changes at 60°N (Winograd et al., 1992). Others, however, interpret DH-11 as a regional climate record supporting the orbital paradigm (Imbrie, 1992; Emiliani, 1993; Shackleton, 1993).

Those involved in the development of proxy records may, at this point, be concerned with issues of uncertainties in the dating of these records and in the dating of the insolation curves. The underlying philosophy behind orbital tuning (c.f. Martinson et al., 1987) assumes that the astronomical cycles are "absolute" in their timing, and that the proxy records must be "accordion-ed" to match. Our approach makes no such assumption. As such, we are susceptible to the inherent errors in the published proxy records. Although we choose not to deal with the error terms in this paper for introductory purposes and computational simplicity, a next step would be to insert the error bars and use chance-constrained programming, a variant of LP that allows one to convert probability distributions to deterministic values (Taha, 1976). Furthermore, we address this issue in another way by considering how time lags affect the results.

### 2.2. *Milankovitch insolation curves*

Many independent solar radiation variables might influence a paleoclimatic record. These insolation variables derive from expansions of the basic astronomical variables, $e$ (eccentricity), $\epsilon$ (obliquity) and $e \sin \varpi$ (precession/eccentricity) (Berger, 1978):

$$\epsilon = \epsilon^* + \sum A_i \cos(f_i t + \delta_i) \quad (1)$$

$$e \sin \varpi = \sum P_i \sin(\alpha_i t + \zeta_i) \quad (2a)$$

$$e \cos \varpi = \sum P_i \cos(\alpha_i t + \zeta_i) \quad (2b)$$

$$e = e_0 + \sum E_i \cos(\lambda_i t + \phi_i) \quad (3)$$

where the constants of integration $\epsilon^*$ and $e_0$are 23.320556° and 0.028707 respectively. The index $i$ refers to the series expansion tables (specifically tables 1–3) given by Berger (1978); the amplitudes $A_i$, $P_i$ and $E_i$, the mean rates $f_i$, $\alpha_i$ and $\lambda_i$ and the phases, $\delta_i$, $\zeta_i$ and $\phi_i$ are taken from those same expansion tables; and $t=0$ refers to 1950 A.D. and is negative for the past. Insolation (in $MJm^{-2}$) is measured as the difference from present day insolation.

We calculated 342 different insolation time series: 19 latitudes × 3 seasons × 3 diurnal classes × 2 mirror images. Latitudinally, we used ten-degree increments from 90°N to 90°S. Seasonally, we calculated insolation at the June solstice, December solstice and March equinox. For each latitude and season, we computed three diurnal components (Cerveny, 1991) by linking the values produced with the Berger parameterizations to the work of Cogley (1979), who categorized radiation as a function of discrete elevation angle. The three classes are (1) total daily insolation; (2) noontime radiation, i.e., the radiation received within five degrees of the highest elevation angle obtained for the given latitude and season and (3) radiation received at times other than that of the noontime class, i.e., total daily radiation minus noontime radiation. These three classes provide a wider array of possibilities to analyze than daily average insolation alone (Cerveny, 1991; Berger et al., 1993). We also computed the mirror image of each radiation time series so as to include the possibility that inverse relationships might contribute to paleoclimatic signals. Each insolation time series goes back 250,000 yr.

Both proxy and insolation datasets were standardized to values between 0 and 1, with the highest value of each series corresponding to 1. This enables the long-term variability in the radiative datasets, rather than the actual totals (which are so much higher in the tropics), to be the critical factor in determining the solutions.

## 3. Linear programming methodology

We aim to find the linear combination of solar insolation curves that best fits a given paleoclimatic

proxy time series curves. In other words, we want to identify the subset of solar insolation curves and weights on each curve such that, when the curves are weighted and added together, the resulting composite curve minimizes, in some fashion, deviations from the proxy curve. Our application of the LP methodology is illustrated graphically in Fig. 1, which shows component by component construction of the composite radiation curve that best fits the Vostok proxy record.

In order to translate this graphical method into mathematics, we must first decide what constitutes the "best fitting" curve. For any dependent variable $Y$, Eq. (1) is a general formula for minimizing the sum of the deviations between $y_t$, the observed value at time $t$, and $\hat{y}_t$, the predicted value, taken to some power $k$ (Zanakis and Rustagi, 1982):

$$\text{Minimize: } \sum_{t=1}^{T} |y_t - \hat{y}_t|^k \qquad (4)$$

In our analyses, the dependent (or response) "$Y$" variable is a paleoclimatic proxy record. The $\hat{y}_t$ are a function of the solar radiation datasets, each of which is an independent (or predictor) "$X$" variable.

Eq. (4) can generate three basic criteria for the best fit, depending on $k$. If $k=2$, the criterion in Eq. (4) minimizes the sum of squared errors. This criterion is known as the $L_2$-norm, or more commonly as "ordinary least squares" (OLS), as used in standard multiple regression analysis. If $k=1$, Eq. (4) yields the minimum sum of the absolute errors, also known as the $L_1$-norm or the "minisum" (Narula, 1982). If $k=\infty$, minimizing Eq. (4) is equivalent to minimizing the maximum absolute error, known as the $L_\infty$-norm or the "minimax." Outliers influence the minisum less than OLS because the deviations are not squared, while the minimax looks only at the largest outlier.

Ordinarily, OLS would be preferred because of its closed-form solution procedure and its well-developed inferential properties that allow statistical significance to be determined. Unfortunately, our dataset violates the assumptions of OLS in several ways. First, the radiation time series are multicollinear, e.g., there is a very high correlation

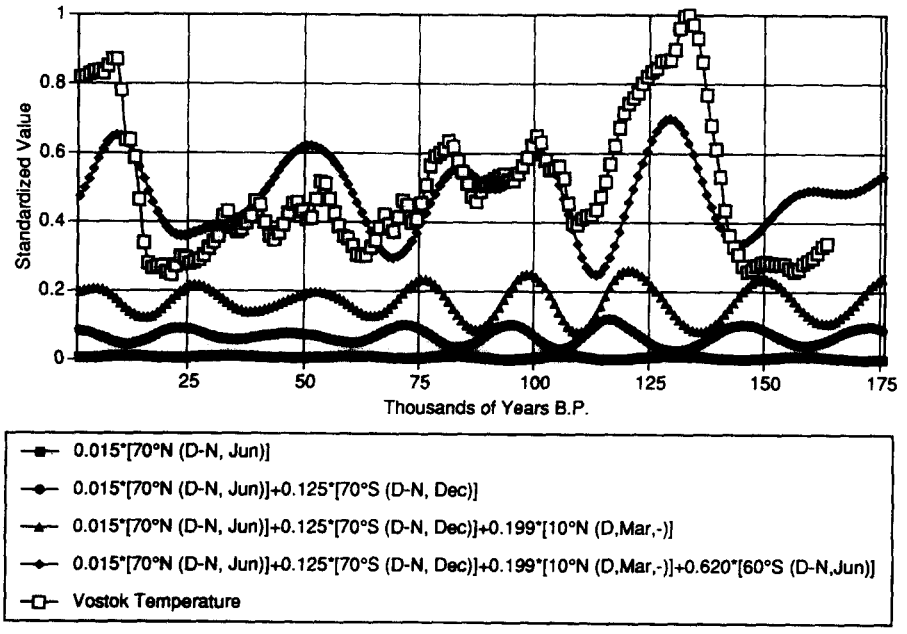


Fig. 1. The method of constructing a composite radiation curve is illustrated for the Vostok record. These four insolation curves comprise the subset that minimizes the average deviation. The make-up of the composite curve is illustrated by weighting and adding the components vertically, in ascending order of their optimal weights. The uppermost curve (with black diamonds) is the final composite insolation curve.

between adjacent radiation curves, such as 60° N and 50° N. Second, each radiation and proxy record time series is temporally autocorrelated; in other words, the values at time $t$ are highly correlated with those at $t-1$. Third, there are more independent variables than there are observations of the dependent variable, unless we were to a priori cut back the number of latitudes, seasons, or times of day.

While there are no closed-form solution methods for these two criteria, LP methods for solving the minisum (Charnes et al., 1955) and minimax (Kelley, 1958) have been known since the 1950s. We solved our LPs using the revised Simplex algorithm (Dantzig, 1951). This methodology is guaranteed to find the global optimum by swapping variables in and out until no swaps remain that would improve the solution. The curve-fitting methods using LP are considered "robust regression" techniques that can be used on matrices of less than full rank (Narula, 1982) — in other words, with multicollinearity, or with a greater number of independent variables than observations. LP curve-fitting has been used in economics for combining multiple forecasts (time series) into a single weighted forecast (Reeves and Lawrence, 1982), and the minisum LP has been found to outperform OLS in most autoregressive models (Cogger, 1989).

Every LP consists of decision variables whose values are to be optimized, an objective function "$Z$" defining optimality, and constraints defining feasibility. In the minisum LP model, the decision variables are the weights $W_{ijk\lambda}$ on the radiation datasets and the positive and negative deviations $d^+$ and $d^-$. The minisum LP is defined as:

$$\text{Minimize: } Z_1 = \sum_{t=1}^{T} [d_t^+ + d_t^-] \tag{5}$$

Subject to:

$$\sum_{i=1}^{19}\sum_{j=1}^{3}\sum_{k=1}^{3}\sum_{\lambda=1}^{2} X_{ijk\lambda t} W_{ijk\lambda} + d_t^+ - d_t^- = Y_t$$

$$\text{for } t = 1,2,3,\ldots T \tag{6}$$

$$W_{ijk\lambda}, d_t^+, d_t^- \geq 0 \tag{7}$$

where:

$d_t^+$, $d_t^-$ positive and negative components of deviation for time $t$

$W_{ijk\lambda}$ weight on the solar insolation dataset for latitude $i=1,\ldots19$; solar angle $j=1, 2, 3$; season $k=1, 2, 3$ and image/mirror image series $\lambda=1, 2$

$X_{ijk\lambda t}$ standardized insolation value for latitude $i$, solar angle $j$, season $k$, image/mirror image series $\lambda$ in time $t$; $0 \leq X_{ijk\lambda t} \leq 1$ for $t=1, 2, 3\ldots T$, in thousands of years

$Y_t$ standardized proxy record value for time $t$; $0 \leq Y_t \leq 1$ for $t=1, 2, 3\ldots T$, in thousands of years

The deviation $d_t$ is broken up into its positive and negative components, $d_t^+$ and $d_t^-$, because LP cannot handle absolute values explicitly. If the $d_t$ variables were allowed to be negative, the minimizing solution would push them all towards $-\infty$. Also, it is worth noting that while Eq. (6) implies that $d_t^+$ and $d_t^-$ could both be nonzero, the objective function Eq. (5) ensures that a better solution can always be found with only one of them nonzero for a given $t$.

In the minimax LP, an additional variable, $d_{\max}$, defined by Eq. (10) to be larger than the absolute value of any deviation, is minimized:

$$\text{Minimize: } Z_2 = d_{\max} \tag{8}$$

Subject to:

$$\sum_{i=1}^{19}\sum_{j=1}^{3}\sum_{k=1}^{3}\sum_{\lambda=1}^{2} X_{ijk\lambda t} W_{ijk\lambda} + d_t^+ - d_t^- = Y_t$$

$$\text{for } t = 1,2,3,\ldots T \tag{9}$$

$$d_t^+ + d_t^- - d_{\max} \leq 0 \text{ for } t = 1,2,3,\ldots T \tag{10}$$

$$W_{ijk\lambda}, d_t^+, d_t^-, d_{\max} \geq 0 \tag{11}$$

Imagine a band of vertical distance $d_{\max}$ above and below the proxy record curve. The minimax problem tries to make a composite radiation curve that stays within the smallest possible band at all times. Thus, in the minimax solution, the location of the composite curve within that band is irrelevant; only the largest deviation matters. In contrast, the minisum model counts all of the deviations equally, but allows a large deviation to

be offset by many small ones. An interesting property of any optimal minimax solution will be that the composite curve will touch the outer edge of the band in at least two places, i.e., there will be at least two absolute deviations equal to $d_{max}$.

LP models are highly flexible, in that they can handle problems in which there are more independent variables than observations. For example, in our models for SPECMAP and *Melosira*, there are 342 independent variables (i.e., weights on insolation time series constructed for each latitude, times of day and season combination), 500 deviation variables, and only 250 observations of the dependent variable. Thus, this approach is ideal for problems with a large number of candidate predictors of a paleoclimatic proxy record.

## 4. Analysis of results

Our purpose in exploring linear programming is to assess its potential as a "screening" tool for sorting through a multitude of variables that could potentially explain a Quaternary dataset. Inherently, this approach is a two-step process. The first step, linear programming, is inductive and purely statistical. In this sense, LP is similar in purpose to stepwise regression, but LP can handle orders of magnitude more variables. However, because purely mathematical analyses can lead to spurious correlations, the first step must be followed by a deductive step that attempts to account for the statistical relationships between the astronomical time series and the proxy record of climate using known physically-based paleoclimatic principles and models (e.g., COHMAP and Members, 1988; Bartlein and Whitlock, 1993). In this paper, the second step will be limited to a preliminary assessment of the biophysical linkages between proxy records and insolation curves selected by LP based on contemporary paleoclimatic paradigms.

Altogether, we ran sixteen LP analyses. In the first eight, each of the four proxy records was fitted to a solution set of insolation parameters using the minisum and minimax models. We ran eight additional LP analyses in which each of the climatic proxy records lagged the insolation datasets by 5000 yr. Lags have been proposed by Broecker and Denton (1989) and Imbrie et al. (1992, 1993a) to explain how feedback mechanisms can delay climatic responses to orbital forcing. Our choice of 5000 yr as the lag length is based on the estimate of Martinson et al. (1987) that the error range in the SPECMAP climatic records averages $\sim \pm 5000$ yr. However, we do not view the specific length of the lag to be as important as how the lag altered results.

### 4.1. How to read the results

The solutions for the four different proxy records are portrayed in Fig. 2a–d in both graphical and tabular form. In each figure, the composite curves generated by the minisum and minimax (lagged and unlagged) LP models are compared visually to the proxy record, shown as a shaded line. At the top of each figure, the identical proxy record is superimposed over the standardized curve for daily total insolation at the June solstice at 60°N — the time series that has been the focus of the Milankovitch paradigm.

Adjacent to each analysis graph in Fig. 2 is a table showing the components (top) and performance (bottom) of each LP solution. The top part provides the latitude, season, time of day, and $\lambda$ value for each component curve, followed by the optimal weight accorded to each curve. For instance, the first component of the Vostok solution is the positive (as opposed to mirror) image of the daily-minus-noon component of the June solstice insolation at 70° N, which is weighted by 0.015.

The bottom half of the table shows the maximum and average residuals. For comparison purposes, the table also shows, in square brackets, the average and maximum residuals for the traditional Milankovitch hypothesis, i.e., the equivalent residuals for the best possible fit between the proxy record and the daily total insolation at 60°N at the June solstice.

### 4.2. Composition of the solution set

It is important to note that *linear combinations* of insolation curves are being matched against the

proxy records, not individual curves. The number of curves selected by the LP methodology as a solution set is an output of the model, not an input. Theoretically, the number of possible solutions is equal to the number of combinations of 342 curves taken one at a time, plus the combinations taken two at a time, three at a time, and so on, up to a solution with all 342 curves participating. The fact that all sixteen of our solutions were comprised of four to five insolation time series (Fig. 2a–d) is significant. First, it means that a combination of several insolation curves fits the proxy record better than any single curve. Second, after the best solution of four to five curves is found, there is no additional benefit to adding more curves, either because they would worsen the correlation or because they would duplicate the variance already explained by the best four or five. It is significant that the solutions consist of four to five curves because (a) it is a manageable number to interpret and (b) a selection of dozens or hundreds of curves would have suggested that the correlations were random. Since similar curves kept being chosen, the correlations are not likely to be happenstance.

The idea of using several insolation time series to explain paleoclimatic phenomena is not completely new. Struck et al. (1993) argued, for example, that insolation changes at different latitudes, interacting in tandem, may be related to global climate change through ocean–atmosphere carbon exchanges. However, most past paleoclimatic studies have considered only a single astronomical time series: June solstice daily insolation around 60°N (e.g., Hays et al., 1976; Berger, 1978; Jouzel et al., 1987; Martinson et al., 1987; Broecker and Denton, 1989; Imbrie, 1992; Imbrie et al., 1992). The justification for this previous focus on 60°N involves complex ocean–atmosphere feedbacks and is not limited to the traditional Milankovitch interpretation that variations in Northern Hemispheric polar insolation drive global ice volume (Broecker and Denton, 1989; Imbrie et al., 1992). Still, the deductive restriction to 60°N carries the assumption that the signal evident in a given paleoclimate proxy record is global.

Our discussion of results falls into two general categories: a general analysis of the distribution of selected weights from all sixteen runs and a more specific analysis of the solution sets for each proxy record.

### 4.3. Generalized analysis of the results

We begin by examining commonality across all sixteen runs. Fig. 3a sums the weights on all curves at 10° latitude intervals from 80°N–80°S. These sums were then disaggregated by type of model (Fig. 3b), season (Fig. 3c) and time of day (Fig. 3d) to see whether any patterns between latitudes and other factors could be discerned.

High latitudes in both North and South Hemispheres dominate the results (Fig. 3a). Because obliquity drives insolation at high latitudes, LP analyses have selected inductively latitudes where obliquity signals are felt the strongest (Liu, 1992). A significant aspect of this finding is that 60° South, not North, is the most heavily weighted latitude. Overall, Southern Hemisphere high latitudes are weighted in twelve, heavily in nine, of the sixteen analyses. This finding is consistent with the observation that:

"The Southern Ocean is the only oceanic domain encircling the globe. It contains the strong eastward flow of the Antarctic Circumpolar Current, and is the unifying link for exchanges of water masses at all depths between the world's major ocean basins. As these exchanges are an important control on mean global climate, the Southern Ocean is expected to play an important role in transmitting climate anomalies around the globe." (White and Peterson, 1996, p. 699)

The importance of insolation at high southern latitudes has been recognized previously (e.g., Imbrie et al., 1992; Struck et al., 1993). There is increasing evidence of interhemispheric linkages based on Antarctic and Greenland ice cores (Mayewski et al., 1996). Southern ocean latitudes may be particularly important in global $CO_2$ fluctuations (Smith and Nelson, 1986; Keir, 1990; Marino et al., 1992), and in interactions between orbital insolation changes, sea ice fluctuations (Crowley and North, 1991), and pathways for the redistribution of heat and salt (Lynch-Stieglitz et al., 1994). It is plausible that insolation changes

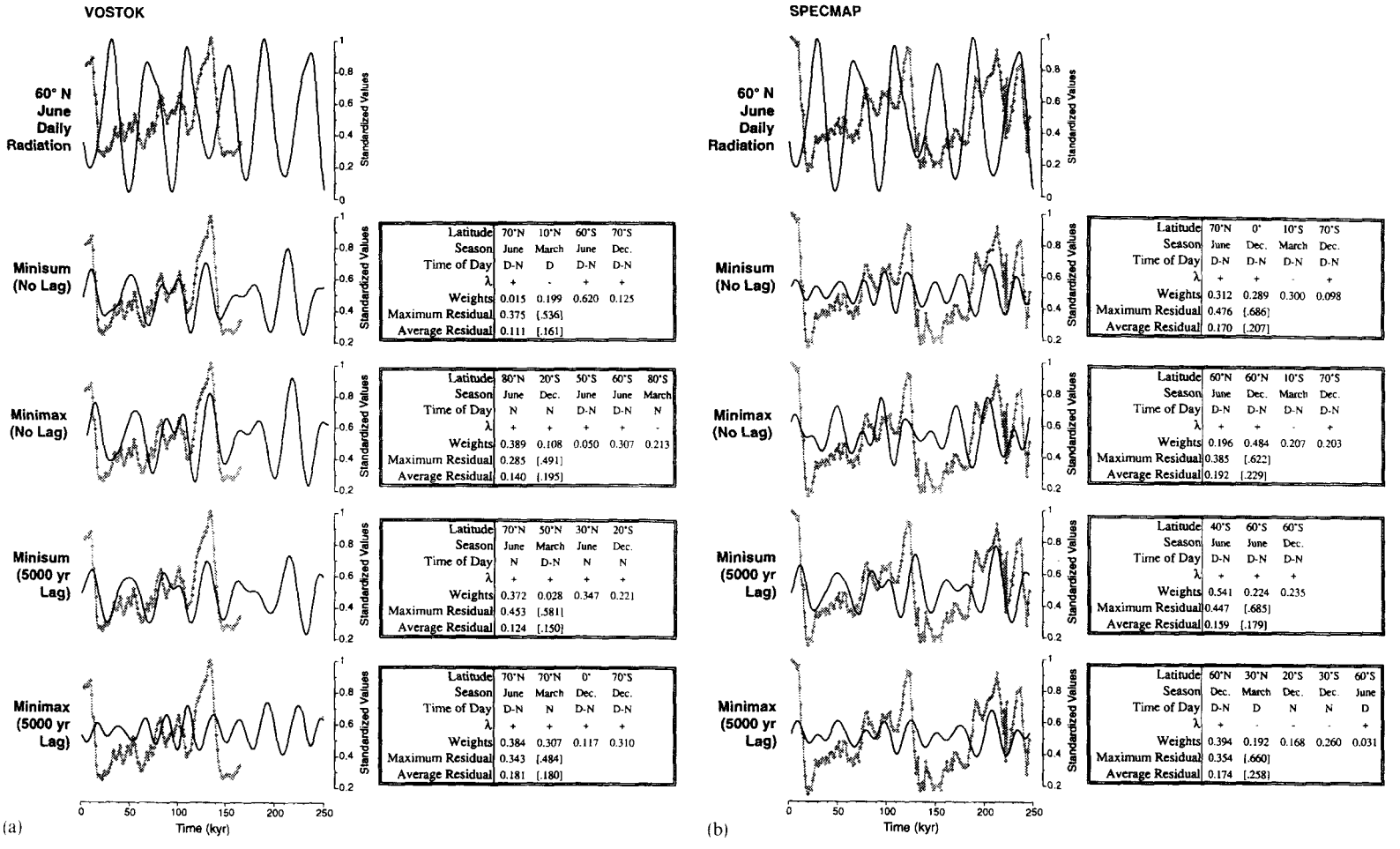


Fig. 2. Analysis results for (a) Vostok, (b) SPECMAP, (c) *Melosira* and (d) Devil's Hole. In each graph, the proxy record is shown by the shaded line, and the composite insolation curve (or the daily June insolation curve at 60°N) is shown by the bold black line. In the accompanying table, the time of day for a component insolation series is given by D = daily, N = noon, and D − N = daily-minus-noon. For λ, the "−" sign indicates the mirror image of the radiation series, while "+" indicates the original series. Accompanying the maximum and average residuals for each model are the corresponding performance measures for daily June insolation at 60°N [in square brackets].

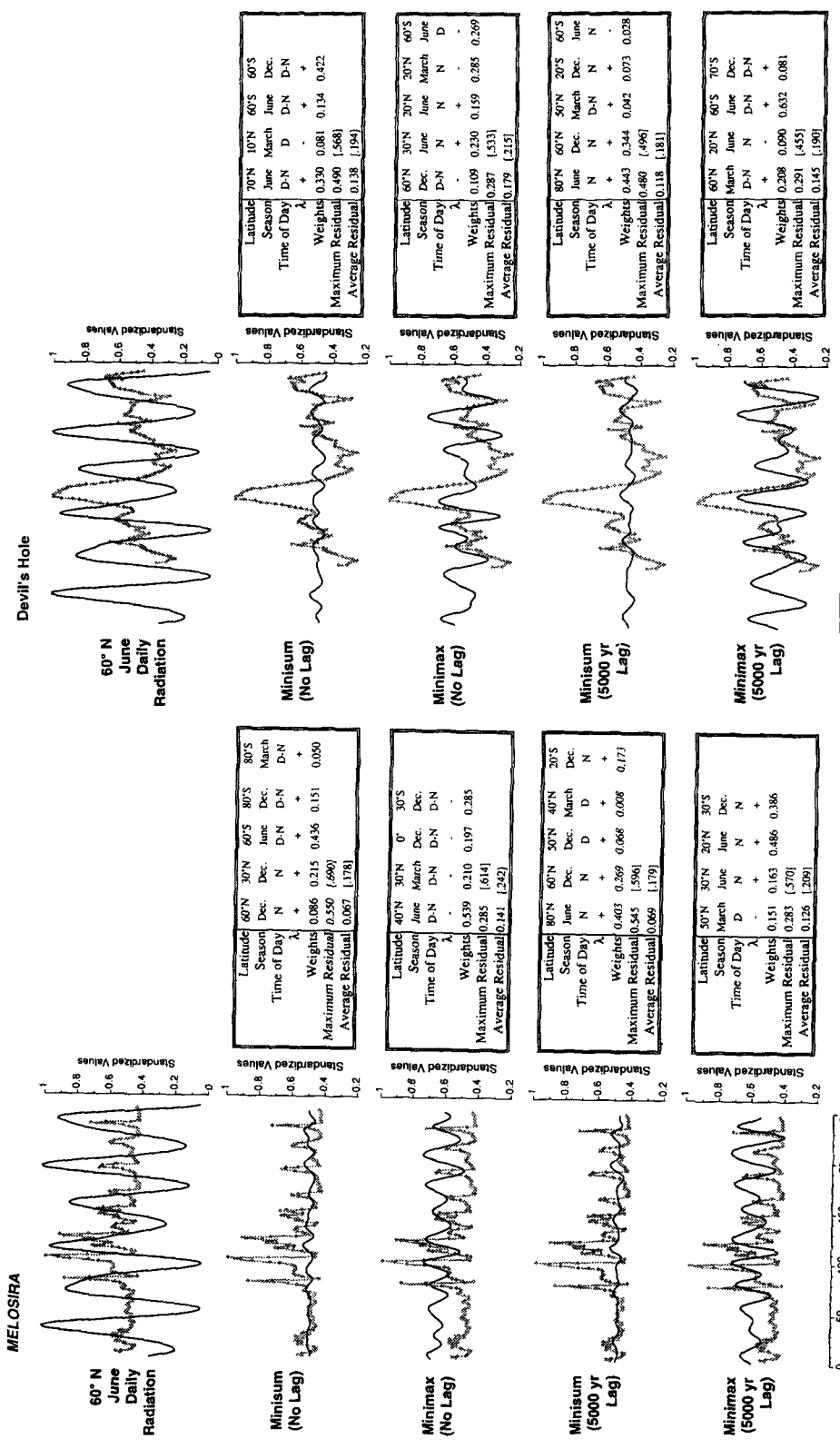


| | 60°N | 30°N | 60°S | 80°S | 80°S |
|---|---|---|---|---|---|
| Season | Dec. | Dec. | June | Dec. | March |
| Time of Day | N | N | D-N | D-N | D-N |
| λ | + | + | + | + | + |
| Weights | 0.086 | 0.215 | 0.436 | 0.151 | 0.050 |
| Maximum Residual | 0.550 | (.690) | | | |
| Average Residual | 0.067 | [.178] | | | |

| | 40°N | 30°N | 0° | 30°S |
|---|---|---|---|---|
| Season | June | March | Dec. | Dec. |
| Time of Day | D-N | D-N | D-N | D-N |
| λ | - | - | - | - |
| Weights | 0.539 | 0.210 | 0.197 | 0.285 |
| Maximum Residual | 0.285 | [.614] | | |
| Average Residual | 0.141 | [.242] | | |

| | 80°N | 60°N | 50°N | 40°N | 20°S |
|---|---|---|---|---|---|
| Season | June | Dec. | Dec. | March | Dec. |
| Time of Day | N | N | D | D | N |
| λ | + | + | + | + | + |
| Weights | 0.403 | 0.269 | 0.068 | 0.008 | 0.173 |
| Maximum Residual | 0.545 | [.596] | | | |
| Average Residual | 0.069 | [.179] | | | |

| | 50°N | 30°N | 20°N | 30°S |
|---|---|---|---|---|
| Season | March | June | June | Dec. |
| Time of Day | D | N | N | N |
| λ | - | + | + | + |
| Weights | 0.151 | 0.163 | 0.486 | 0.386 |
| Maximum Residual | 0.283 | [.370] | | |
| Average Residual | 0.126 | [.209] | | |

| | 70°N | 10°N | 60°S | 60°S |
|---|---|---|---|---|
| Season | June | March | June | Dec. |
| Time of Day | D-N | D | D-N | D-N |
| λ | + | - | + | + |
| Weights | 0.330 | 0.081 | 0.134 | 0.422 |
| Maximum Residual | 0.490 | [.568] | | |
| Average Residual | 0.138 | [.194] | | |

| | 60°N | 30°N | 20°N | 60°S |
|---|---|---|---|---|
| Season | Dec. | June | June | March |
| Time of Day | D-N | N | N | N |
| λ | - | + | + | - |
| Weights | 0.109 | 0.230 | 0.159 | 0.283 |
| Maximum Residual | 0.287 | [.533] | | |
| Average Residual | 0.179 | [.215] | | |

| | 80°N | 60°N | 50°N | 20°S | 60°S |
|---|---|---|---|---|---|
| Season | June | Dec. | March | Dec. | June |
| Time of Day | N | N | D-N | N | N |
| λ | + | + | + | + | - |
| Weights | 0.443 | 0.344 | 0.042 | 0.073 | 0.028 |
| Maximum Residual | 0.480 | (.496) | | | |
| Average Residual | 0.118 | [.181] | | | |

| | 60°N | 20°N | 60°S | 70°S |
|---|---|---|---|---|
| Season | March | June | June | Dec. |
| Time of Day | D-N | N | D-N | D-N |
| λ | + | - | + | + |
| Weights | 0.208 | 0.090 | 0.632 | 0.081 |
| Maximum Residual | 0.291 | [.455] | | |
| Average Residual | 0.145 | [.190] | | |

Fig. 2. (cont.)

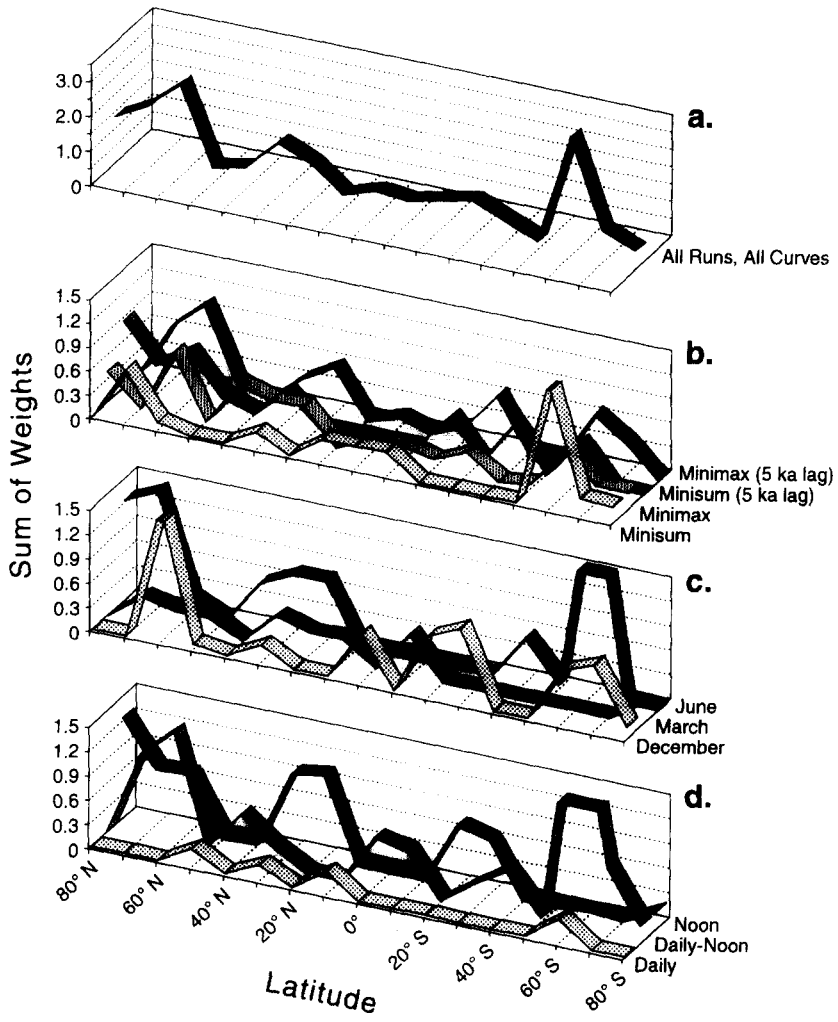


Fig. 3. LP weights on radiation curves, summed over all sixteen analyses, are shown by latitude (a). The results are further disaggregated (b) by model type; (c) by season and (d) by time of day.

at these latitudes could trigger these processes. Imbrie et al. (1992) note that in southern oceans, the "carbon trapping mechanism is driven by a northward shift in the latitude of the maximum southern hemisphere westerlies," which in turn could be partially driven by a radiation-related intensification of Antarctica's thermal gradient.

Low latitudes also appear in LP solutions (Fig. 3a), and the strongest low latitude signal rest at 30°N and 30°S (Fig. 3a). These latitudes correspond with the normal position of the subtropical jet streams, important agents in monsoonal flows and delivering tropical moisture (Reiter, 1963; Arkin, 1982). Although radiation at tropical and equatorial latitudes have been viewed traditionally as less important for driving global climate, recent evidence has challenged that view (Rea et al., 1986; Pisias and Rea, 1988; Clemens et al., 1991; McKenzie, 1993; Karl and Tilbrook, 1994). Struck et al. (1993), for example, point to the east Atlantic equatorial upwelling belt as an important "biological pump" with changes driven by precession. Chappallaz et al. (1993) point to synchronous changes in atmospheric methane in the Greenland and Antarctic ice cores, but driven by changes in low-latitude wetlands.

Daily insolation is virtually the only insolation time series that gets compared with paleoclimatic records (e.g., Hays et al., 1976; Berger, 1978; Jouzel et al., 1987; Martinson et al., 1987; Broecker and Denton, 1989; Imbrie, 1992; Imbrie et al., 1992). Yet, of the three times of day, daily insolation ranked a distant third (Fig. 3d). The daily-minus-noon class dominates a majority of the LP analyses, followed by noontime insolation. Previous studies (Cerveny, 1991; Berger et al., 1993) have shown strong obliquity signals in noontime insolation, while precessional cycles, and to a lesser degree those of eccentricity, control the insolation received at other times of the day. A link between diurnal classes of radiation and climate is plausible, based on two lines of reasoning. First, many of the physical processes linking insolation to climate are influenced by time of day. Because of its low elevation angle, non-noontime radiation evaporates less water from oceans (Cogley, 1979) and ablates less snow and ice (Wiscombe and Warren, 1980) than overhead insolation. Second, prior studies have linked different proxy records to precession (e.g., Pokras and Mix, 1987; Imbrie et al., 1992) and obliquity (e.g., Struck et al., 1993). Precession is tied to daily-minus-noon radiation, which is the most heavily weighted insolation class. In contrast, obliquity drives variability in noontime radiation, which is heavily weighted at subtropical latitudes (Fig. 3d). Interestingly, noontime radiation is heavily weighted at northern polar latitudes, but is almost never selected at southern polar latitudes. This suggests that extensive Northern Hemispheric landmasses respond more to axial tilt variations and subsequent fluctuations in insolation than their maritime counterparts in the Southern Hemisphere.

Our last general point relates to differences between nonlagged and lagged solution sets. As noted earlier, the selection of a 5000 yr lag for the minisum and minimax models was based on Martinson et al. (1987, p. 14); but our purpose in inserting the lag was to see if the solution sets varied, and in what way. Aggregate differences, averaged over the 4 proxy records, are minimal (see Table 1). However, both SPECMAP and Devil's Hole are better represented by lagged data. SPECMAP Terminations I and II are led by lagged composite curves (Fig. 2b). Vostok is best represented by nonlagged models (Fig. 2a). Nonlagged and lagged solution sets consistently included similar polar and mid-latitude groups, but lagged solutions emphasized 20°S–30°S while nonlagged solutions picked equatorial latitudes (Fig. 3b). The decision whether to lag, and if so by how many years, could be based upon an understanding of biophysical processes. Alternatively, it could be part of the inductive search process.

### 4.4. Comparison to June daily 60°N

Although the models are free to choose any and all of the 342 insolation time series, June radiation for high northern latitudes is often chosen by LP to fit the four proxy records. However, composite curves from different latitudes and seasons performed significantly better than June daily 60°N insolation by itself. The poor performance of June daily 60°N is indicated by both lower average residuals in the minisum solutions and lower maximum residuals in the minimax solutions — compared with the same residuals when the models are constrained to select only June solstice daily insolation at 60°N. Overall, in the eight minisum analyses (rows 1 and 3 in Table 1), the average residual for the June daily 60°N solutions was 48% higher than for the composite LP solutions. The difference was even more pronounced in the eight minimax analyses, where the maximum residual for 60°N June daily was, on average, 76% higher. This dramatic improvement suggests individuals who compare paleoclimatic data to insolation may be limiting their analysis by only making comparisons with daily subarctic summer insolation.

### 4.5. Discussion of results for individual proxy records

*Vostok.* Of all the composite curves matched against the various proxy records, the best "visual" match is between nonlagged solutions and the Vostok record (Fig. 2a). The positions of marine oxygen-isotope stages 2, 4, 5b, 5d and 6 are well placed. Terminations I and II are led by or coincide with the composite insolation time series created by LP. Both non-lagged models weight high lati-

Table 1
Comparison of LP model fit with 60°N June daily radiation, by model type and proxy record

| | | Average residual | | Maximum residual | |
|---|---|---|---|---|---|
| | | LP Model | 60°N June daily[a] | LP Model | 60°N June daily[a] |
| Type of model | | | | | |
| | Minisum | 0.122 | 0.185 | 0.473 | 0.620 |
| | Minimax | 0.163 | 0.220 | 0.310 | 0.565 |
| | Minisum (5000 yr lag) | 0.118 | 0.172 | 0.481 | 0.590 |
| | Minimax (5000 yr lag) | 0.157 | 0.209 | 0.318 | 0.542 |
| Proxy record[b] | | | | | |
| | Vostok | 0.139 | 0.172 | 0.364 | 0.523 |
| | SPECMAP | 0.174 | 0.218 | 0.449 | 0.663 |
| | *Melosira* | 0.101 | 0.202 | 0.415 | 0.617 |
| | Devil's Hole | 0.145 | 0.195 | 0.387 | 0.513 |
| All sixteen runs | | 0.140 | 0.197 | 0.403 | 0.579 |

[a]"60°N June Daily" represents solutions in which the June daily total radiation at 60°N was the only independent variable. The weight was optimized so as to minimize either the maximum or average residual.
[b]Comparisons between proxy records are not recommended because, although all the proxy records were standardized for a mean of 0.5 and a maximum of 1.0, they do not all have the same total variation.

tudes in the Southern Hemisphere heavily, which is consistent with the geographic position of the Vostok record.

Although heavy weightings on Southern Hemisphere insolation curves for Vostok argue against a spurious selection, the particular southern insolation curves selected were surprising to us. The model with the lowest average residual, the minisum (no lag) model, weights most heavily on daily-minus-noon curves at high southern latitudes. The high weight for June at 60°S was the most surprising, given the low radiation totals. But then again, the threshold for climatic response to insolation is unknown. The equinox signal is heavily weighted in noontime radiation at 80°S.

*SPECMAP.* As measured by either the average or maximum residual, the method's fit to SPECMAP is worse than that for any other proxy (Table 1). Nonetheless, our composite curves still fit SPECMAP much better than 60°N June daily insolation by itself (see Fig. 2b). We speculate that LP's relatively poor fit may be due to the way SPECMAP was constructed from many locations. Also, the models in which data were lagged by 5000 yr fit better than their nonlagged counterparts. We speculate that this may relate to differences in response rates to insolation changes of global scale as opposed to local scale.

Given its composite construction, we would anticipate that SPECMAP, in contrast to the other proxy records, would be more strongly influenced by the latitudes that control a global signal. We note that June daily insolation at 60°N appears in none of the SPECMAP solutions, despite the fact that it is the insolation signal to which SPECMAP is "orbitally tuned." To explain this, we note that "orbital tuning" adjustments attempt to match specific peaks or valleys of the proxy record to matching peaks and valleys of the insolation curve. In contrast, our LP method covers every reading at 1000 yr intervals, and consequently must also try to fit the slopes between the peaks and valleys.

Arctic (and Antarctic) latitudes *are* prominent in the SPECMAP results, but the insolation curves chosen are for the daily-minus-noon time period. Of the four models for SPECMAP, minisum-lag has the lowest average residual, the best visual fit, and its composite insolation curve peaks slightly in advance of most of the major global paleoclimatic trends visible in the SPECMAP record. The heavy weighting on 40°S in winter would suggest the importance of low sun angle insolation changes over the southern ocean – – a combination that has not yet been explored in paleoclimatic research, but might be related to the Antarctic Circumpolar Wave (White and Peterson, 1996).

*Melosira.* The *Melosira* solutions have lower average residuals than for any other proxy record — and yet visually, the minimax solutions seem to fit it better than the minisum ones (Fig. 2c). This is almost surely an artifact of there being less total variation in the *Melosira* record, which stays relatively stable in the 0.4–0.5 range except for sharp spikes of short duration produced by a nonlinear desiccation process (Pokras and Mix, 1987). The minisum model adapts to the shape of this curve by fitting a very flat curve to its stable base level. *Melosira*'s shape is best modeled using a minimax formulation, which cannot ignore the spikes (i.e., desiccation events) because its objective function criteria is to minimize the single worst outlier.

The minimax model with the 5000 yr lag best fits the *Melosira* dataset (Table 1). The prominent low-latitude insolation weights in this solution set are consistent with the record's tropical location. Here, summer solstice noon radiation around the tropics of Cancer and Capricorn are weighted most heavily. This would be consistent with the explanation of variations in the supply of moisture being responsible for tropical lake-level fluctuations (Pokras and Mix, 1987). The mid-latitude signals included in both minimax solution sets could be the result of atmospheric dynamics (Gasse et al., 1990).

*Devil's Hole.* LP does not fit DH-11 as well as Vostok or *Melosira* (Fig. 2d). The record is marked by one very large long-lasting spike and several smaller peaks. As a result, the minisum model does not match the peaks and troughs well. However, the minimax (5000 yr lag) model coincides well with the controversial DH-11 Termination II (Winograd et al., 1992; Imbrie, 1992; Imbrie et al., 1993b; Shackleton, 1993) (Fig. 2d).

Young and Bradley (1984) conclude that insolation gradients are important in driving global circulation and in transporting moisture from the mid-latitudes to high latitudes. Since our LP methodology is not designed to analyze gradients, it may be possible that the controlling orbital signal in the DH-11 record (Imbrie et al., 1993a) could not be selected. However, the subtropical latitudes (10°N–30°N) in the DH-11 solution set may point to the importance of these latitudes as the region that supplies moisture for the Nevada hydrologic record. Still, the dominant weights rest with the polar latitudes, which may relate to the polar front as a control on circulation in the southwestern United States, or to Devil's Hole being a truly global signal, as Winograd et al. (1992) have argued.

*Summary of individual proxy records.* A distinct latitudinal pattern can be seen in the results for each proxy record. We calculated the average weighted latitude and the average weighted absolute value of the latitude for each proxy record (Table 2). The former shows the hemispheric bias of the solution, while the latter shows the polar/equatorial bias. Of the four proxy records, three have average weighted latitudes near the Equator; only the *Melosira* solutions have a distinct northerly (11.2°N) average. Given that the *Melosira* record is the most regional of the four, this is not surprising. Vostok, Devil's Hole and SPECMAP, on the other hand, are purported to be global records.

The average weighted absolute latitudes, on the other hand, show that high latitudes explain much more of the Vostok and Devil's Hole records than of *Melosira*. The Vostok record at ~80°S, would be expected to have the highest average absolute latitude. Devil's Hole is taken from the next highest latitude — 35°N — while *Melosira* is a tropical signal from the neighborhood of 15°N. The ordering of the average weighted absolute latitudes in their solution sets — |57°|, |50°| and |42°| — is consistent with the relative ordering of their actual absolute latitudes. The SPECMAP proxy record,

Table 2
Latitudinal comparison, by proxy record

| | Weighted average latitude | Weighted average Absolute value of latitude |
|---|---|---|
| Vostok | 1.99°N | 56.56° |
| Devil's Hole | 0.42°N | 50.33° |
| *Melosira* | 11.20°N | 41.99° |
| SPECMAP | 0.90°N | 43.63° |

compiled as it were from a global database, must be excluded from this type of comparison.

Although the relationship between the latitude of the proxy records and the latitudes of the insolation curves selected by the LP is clear, some might have expected the relationship to be stronger. However, the general circulation of the atmosphere and the oceans transfers substantial energy, and we would be disturbed if the LP method developed a perfect match with the proxy records' latitudes. Proxy records should be noisy because they record only a portion of the climate signal. Sudden and dramatic climatic changes are not necessarily driven by insolation variations (Broecker, 1994) and would add noise to a record that might otherwise measure insolation variability. Consequently, biophysical indicators record only a part of the climate signals, as, for instance, inflation is only one indicator of the state of an economy.

## 5. Correlation vs. causation

Inductive LP analysis by itself, in the absence of any physical process theory, runs the unavoidable risk of selecting time series which may have nothing to do with the proxy record, but which, when added together, happen to fit the proxy series closely. The "null hypothesis" to this paper is that these solutions are nothing more than happenstance correlation. We are concerned about the purely random null hypothesis and the lack of an available test of statistical significance.

Despite these concerns, we feel that several pieces of evidence strongly suggest that the correlations we found have some biophysical bases. First, all latitudes were not represented evenly, as might have been expected from a random process. Second, daily insolation curves were almost completely excluded from the LP solution sets. Third, both high latitudes and daily-minus-noon insolation — which dominate the LP solutions — have been linked to obliquity and precessional signals respectively. Fourth, the weighted averages of the latitudes chosen by LP for the Vostok, *Melosira* and Devil's Hole proxy records are clearly related to the latitudes of their source regions. A random selection could not produce these four patterns.

Out of 342 possible insolation curves to choose from, only 42 unique curves were selected in any of the 16 runs, and of these, only twelve curves — less than four percent of the total number of possible predictors — were selected more than once. The "top four" single insolation curves accounted for 29% of the combined weights of the sixteen solution sets. The top four curves were: daily-minus-noon radiation in June at 60°S (six times); daily-minus-noon radiation in December at 70°S (five times); daily-minus-noon radiation in June at 70°N (four times) and noon radiation in December at 20°S (four times). Four insolation curves out of 342 possible choices would not account for nearly a third of the weights had the selections been random.

## 6. Conclusions

A perusal of various Quaternary publications reveals a frequently attempted correlation: comparing paleoclimatic proxy records to a single insolation times series, most typically 60°N June daily insolation. Methodologically, LP offers paleoclimatologists a new inductive approach to link a particular climatic proxy dataset with a large number of potential forcings, illustrated here with 342 insolation series. LP's greatest utility stems from its ability to screen a large number of potential predictor series, not to mention the far larger number of all possible combinations of such predictor series. While a researcher may have deductive reasons to believe that a particular forcing might have driven a particular proxy record, other space–time combinations might fit the proxy record much better.

While the deductive approach is admittedly *the* scientific method for testing a theory, it is widely recognized that inductive approaches sometimes play an important role in the actual ebb and flow of scientific discovery, as in the seminal work by Hays et al. (1976). The inductive–deductive linkage can work forwards, as we have done here, or backwards. As shown here for astronomical time series, inductive LP analysis can identify climati-

cally important latitudes, seasons and times of day. These in turn provide a beginning point for in-depth deductive analysis of the specific climatic processes that might have translated fluctuations in insolation into the response that left its mark on the proxy record. On the other hand, if deductive theorizing is done first, inductive LP analysis can then identify specific datasets that may best represent those processes, much as factor analysis is used to reduce data complexity in multivariate statistics.

In this paper, we objectively found combinations of radiation curves for latitudes and times other than 60°N June solstice daily total that fit the proxy records, on average, 40% better as measured by the average or maximum residuals (see Table 1). We have coupled our improved curve-fittings with plausible process-oriented, deductive explanations to reach the following conclusions:

First, the heavy weighting of Antarctic insolation curves in fitting all of the proxy records may suggest the global importance of the southern oceans. Second, our inductive analyses reinforce the deductive notion voiced by many scientists that local or regional climatic processes cannot be ignored in analyzing the causes of a given proxy record (Pokras and Mix, 1987; Bartlein and Whitlock, 1993; Emiliani, 1993; Imbrie et al., 1993a). Third, June insolation at 60°N is one of the prominent signals selected. However, our findings suggest that 60°N does not account for global or regional records nearly as well as a combination of insolation from different latitudes, seasons, and angles. Fourth, daily-minus-noon and noon insolation curves dominate all of the sixteen analyses, which suggests that individual astronomical mechanisms, in this case obliquity (noon) and precession (daily-minus-noon), are more influential in accounting for proxy variations than the orbital effects recorded in total daily insolation. Fifth, lagged data fit better to Devil's Hole and SPECMAP proxies, which could possibly suggest that these proxies may be more affected by feedback-delay processes than the Vostok or *Melosira* records.

Finally, the different proxy datasets yielded different findings, which exemplify the potential of LP as a searching tool. First, the Vostok solution, weighted most heavily by Antarctic and subantarctic insolation curves, had the highest average weighted absolute latitude. Visually, the match between the composite insolation curve and the proxy record was better for Vostok than for any of the other three proxy records. Second, of the four proxy records, LP produced the worst fit for SPECMAP, which is surprising given that it is orbitally tuned. Third, the prevalence of low-latitude Northern Hemisphere insolation curves in *Melosira*'s solution set gave it the lowest average weighted absolute latitude of any of the four proxy records, while at the same time making it the only proxy record with an average weighted latitude substantially north of the Equator. Also, the high kurtosis in the *Melosira* dataset highlighted the difference between the optimization criteria for the minisum and minimax models. Fourth, the weighted average of the absolute latitudes for the Devil's Hole solutions fell, as expected, in between those of the more polar Vostok record and the more equatorial *Melosira* record. Furthermore, we note that Devil's Hole best fitting composite curve, the minimax (5000 yr) lag model, coincides well with the controversial Termination II.

LP models are not limited to fitting time series, but could be used in almost any situation where regression is called for, but the assumptions of OLS are violated. Quaternary research is filled with "polygenetic" systems — where the state measured by a proxy record at any given place could be produced by different combinations of a large number of variables. LP is a tool that may offer new insights into complex Quaternary phenomena.

More philosophically, paleoclimatology is undergoing a paradigm shift, away from the universality of orbital forcings and towards an increased appreciation of nonlinear sudden and dramatic climatic changes over millennial time scales (Behl and Kennett, 1996; Hughen et al., 1996; Sirocko et al., 1996). Shifts in perspectives are a healthy and exciting part of deductive analysis. Yet, an important reason for utilizing inductive tools, such as LP, is to bypass paradigm biases (as much as possible). For example, a next step could be to add iceberg releases (Broecker, 1994) or

volcanic eruptions (Zielinski et al., 1996) or other non-cyclical forcings to the selection process. Or for future work, other LP curve-fitting models, such as extensions of minisum and minimax, may yield additional insights (Narula and Wellington, 1979; Reeves and Lawrence, 1982). The very existence of the ongoing paradigm debate in paleoclimatology speaks to the need for an inductive tool to help sort through innumerable possible forcings.

## Acknowledgements

We thank Pat Bartlein, Brian Atwater and an anonymous reviewer for helpful comments, and Alan Mix for core V30-40 dataset. The "SPECMAP" and "Vostok" datasets were obtained from the National Geophysical Data Center in Boulder, Colorado. We thank B. Trapido-Lurie for graphical support and J. Shaffer for digitizing the DH-11 record. R. Daniel of Dash Associates Ltd. provided technical support and consulting. R.C. received partial support from NSF grant SES 9121398. M.K. and R.D. thank Arizona State University for sabbatical support.

## References

Anderson, D.J., Bishop, F. and Lindsley, D., 1991. Internally consistent solution models for Fe–Mg–Mn–Ti oxides: Fe–Mg–Ti oxides and olivine. Am. Mineral., 76: 427–444.

Arkin, P.A., 1982. The relationship between interannual variability in the 200 mb tropical wind field and the Southern Oscillation. Mon. Weather Rev., 110: 1393–1404.

Bartlein, P.J. and Whitlock, C., 1993. Paleoclimatic interpretation of the Elk Lake pollen record. Geol. Soc. Am. Spec. Pap., 276: 275–283.

Behl, R.J. and Kennett, J.P., 1996. Brief interstadial events in the Santa Barbara basin, NE Pacific, during the past 60 kyr. Nature, 379: 243–246.

Berger, A., 1978. Long-term variations of daily insolation and Quaternary Climatic Changes. J. Atmos. Sci., 35: 2362–2367.

Berger, A., Loutre, M.F. and Tricot, C., 1993. Insolation and Earth's orbital periods. J. Geophys. Res., 98: 10,341–10,362.

Broecker, W.S., 1994. Massive iceberg discharges as triggers for global climate change. Nature, 372: 421–424.

Broecker, W.S. and Denton, G.H., 1989. The role of ocean–atmosphere reorganizations in glacial cycles. Geochim. Cosmochim. Acta, 53: 2465–2501.

Brüggemann, W., 1992. A minimal cost function method for optimizing the age–depth relation of deep sea sediment cores. Paleoceanography, 7: 467–487.

Cerveny, R.S., 1991. Orbital signals in the diurnal cycle of radiation. J. Geophys. Res., 96(D9): 17,209–17,215.

Chappallaz, J., Blunier, T., Raynaud, D., Barnola, J.M., Schwander, J. and Stauffer, B., 1993. Synchronous changes in atmospheric $CH_4$ and Greenland climate between 40 and 8 kyr BP. Nature, 366: 443–445.

Charnes, A., Cooper, W.W. and Ferguson, R.O., 1955. Optimal estimation of executive compensation by linear programming. Manage. Sci., 1: 138–150.

Clemens, S., Prell, W., Murray, D., Shimmield, G. and Weedon, G., 1991. Forcing mechanisms of the Indian Ocean monsoon. Nature, 353: 720–725.

Cogger, K., 1989. Time series analysis and forecasting with an absolute error criterion. In: S. Makridakis and S.C. Wheelwright (Editors), Time Series Analysis and Forecasting with an Absolute Error Criterion. North-Holland, Amsterdam, pp. 189–201.

Cogley, J.G., 1979. The albedo of water as a function of latitude. Mon. Weather Rev., 107: 775–781.

COHMAP and Members, 1988. Climatic changes of the last 18,000 years: Observations and model simulations. Science, 241: 1043–1052.

Crowley, T.J. and North, G.R., 1991. Paleoclimatology. Oxford University Press, New York.

Dantzig, G., 1951. Maximization of a linear function of variables subject to linear inequalities. In: T.C. Koopmans (Editor), Activity Analysis of Production and Allocation. Wiley, New York, pp. 339–347.

Dykstra, D.P., 1984. Mathematical Programming for Natural Resource Management. McGraw-Hill, New York.

Emiliani, C., 1993. Milankovitch theory verified. Nature, 364: 583–584.

Gasse, F., Tehet, R., Durand, A., Gilbert, E. and Fontes, J.-C., 1990. The arid–humid transition in the Sahara and the Sahel during the last deglaciation. Nature, 346: 141–146.

Hays, J.D., Imbrie, J. and Shackleton, N.J., 1976. Variations in the earth's orbit: Pacemaker to the ice ages. Science, 194: 1121–1132.

Hughen, K.A., Overpeck, J.T., Peterson, L.C. and Trumbore, S., 1996. Rapid climate changes in the tropical Atlantic region during the last deglaciation. Nature, 380: 51–54.

Imbrie, J., 1992. Editorial: A good year for Milankovitch. Paleoceanography, 7: 687–690.

Imbrie, J., Berger, A., Boyle, E.A., Clemens, S.C., Duffy, A., Howard, W.R., Kukla, G., Kutzbach, J., Martinson, D.G., McIntyre, A., Mix, A.C., Molfino, B., Morley, J.J., Peterson, L.C., Pisias, N.G., Prell, W.L., Raymo, M.E., Shackleton, N.J. and Toggweiler, J.R., 1993a. On the structure and origin of major glaciation cycles: 2. The 100,000-year cycle. Paleoceanography, 8: 699–735.

Imbrie, J., Boyle, E.A., Clemens, S.C., Duffy, A., Howard, W.R., Kukla, G., Kutzbach, J., Martinson, D.G., McIntyre, A., Mix, A.C., Molfino, B., Morley, J.J., Peterson, L.C., Pisias, N.G., Prell, W.L., Raymo, M.E., Shackleton, N.J. and Toggweiler, J.R., 1992. On the structure and origin of

major glaciation cycles: 1. Linear responses to Milankovitch forcing. Paleoceanography, 7: 701–738.

Imbrie, J. and Imbrie, J.Z., 1980. Modelling the climatic response to orbital variations. Science, 207: 943–953.

Imbrie, J., Mix, A.C. and Martinson, D.G., 1993b. Milankovitch theory viewed from Devils Hole. Nature, 363: 531–533.

Jouzel, J., Lorius, C., Petit, J.R., Genthon, C., Barkov, N.I., Kotlaykov, V.M. and Petrov, V.M., 1987. Vostok ice core: a continuous isotope temperature record over the last climate cycle (160,000 years). Nature, 329: 403–408.

Kachroo, R.K., 1992. River flow forecasting: Part 1, a discussion of the principles. J. Hydrol., 133: 1–15.

Karl, D.M. and Tilbrook, B.D., 1994. Production and transport of methane in oceanic particulate matter. Nature, 368: 732–734.

Keene, A.S., 1981. Prehistoric Foraging in a Temperate Forest: A Linear Programming Model. Academic Press, New York.

Keir, R.S., 1990. Reconstructing the ocean carbon system variation during the last 150,000 years according to the Antarctic nutrient hypothesis. Paleoceanography, 5: 253–276.

Kelley, J.E., 1958. An application of linear programming to curve fitting. J. Appl. Math., 6: 15–22.

Leinen, M. and Pisias, N., 1984. An objective technique for determining end-member compositions and for partitioning sediments according to their sources. Geochim. Cosmochim. Acta, 48: 47–62.

Liu, H.-S., 1992. Frequency variations of the Earth's obliquity and the 100-kyr ice-ages cycles. Nature, 358: 397–399.

Ludwig, K.R., Simmons, K.R., Szabo, B.J., Winograd, I.J., Landwehr, J.M., Riggs, A.C. and Hoffman, R.J., 1992. Mass-Spectrometric $^{230}Th$–$^{234}U$–$^{238}U$ dating of the Devils Hole calcite vein. Science, 258: 284–287.

Lynch-Stieglitz, J., Fairbanks, R.G. and Charles, C.D., 1994. Glacial–interglacial history of Antarctic intermediate water: relative strengths of Antarctic versus Indian Ocean sources. Paleoceanography, 9: 7–29.

Marino, B.D., McElroy, M.B., Salawitch, R.J. and Spaulding, W.G., 1992. Glacial-to-interglacial variations in the carbon isotopic composition of atmospheric $CO_2$. Nature, 357: 461–466.

Martinson, D.G., Pisias, N.G., Hays, J.D., Imbrie, J., Moore, T.C. and Shackleton, N.J., 1987. Age dating and the orbital theory of the ice ages: Development of a high-resolution 0–300,000 year chronostratigraphy. Quat. Res., 27: 1–29.

Mayewski, P.A. et al., 1996. Climate change during the last deglaciation in Antarctica. Science, 272: 1636–1638.

McKenzie, J.A., 1993. Pluvial conditions in the eastern Sahara following the penultimate deglaciation: implications for changes in atmospheric circulation patterns with global warming. Palaeogeogr., Palaeoclimatol., Palaeoecol., 103: 95–105.

Narula, S.c., 1982. Optimization techniques in linear regression: a review. TIMS Studies Manage. Sci., 19: 11–29.

Narula, S.C. and Wellington, J.F., 1979. Selection of variables in linear regression using the minimum sum of weighted absolute errors criterion. Technometrics, 21: 299–306.

Pisias, N. and Rea, D.K., 1988. Late Pleistocene paleoclimatology of the central equatorial Pacific: sea surface response to the southeast trade winds. Paleoceanography, 3: 21–37.

Pokras, E.M. and Mix, A.C., 1987. Earth's precession cycle and Quaternary climate changes in tropical Africa. Nature, 326: 486–487.

Rea, D.K., Chambers, L., Chuey, J., Janecek, T., Leinen, M. and Pisias, N., 1986. A 420,000-year-record of cyclicity in oceanic and atmospheric processes from the eastern equatorial Pacific. Paleoceanography, 1: 577–586.

Reeves, G.R. and Lawrence, K.D., 1982. Combining multiple forecasts given multiple objectives. J. Forecasting, 1: 271–279.

Reiter, E.R., 1963. Jet Stream Meteorology. University of Chicago Press.

Shackleton, N.J., 1993. Last interglacial in Devil's Hole. Nature, 362: 596.

Shannon, R.E., Long, S.S. and Buckles, B.P., 1980. Operations research methodologies in industrial engineering: a survey. AIIE Trans., 12: 364–367.

Sirocko, F., Garbe-Schönberg, D. and Molfino, B. 1996. Teleconnections between the subtropical monsoons and high-latitude climates during the last deglaciation. Science, 272: 526–529.

Smith, W.O., Jr. and Nelson, D.M., 1986. Importance of ice edge phytoplankton blooms in the Southern Ocean. BioScience, 36: 251–257.

Struck, V., Sarntein, M., Westerhausen, L., Barnola, J.M. and Raynaud, D., 1993. Ocean–atmosphere carbon exchange: Impact of the "biological pump" in the Atlantic equatorial upwelling belt over the last 330,000 years. Palaeogeogr., Palaeoclimatol., Palaeoecol., 103: 41–56.

Taha, H.A., 1976. Operations Research. MacMillan, New York.

Thomas, G. and DaCosta, J., 1979. A sample survey of corporate operations research. Interfaces, 9: 102–111.

White, W.B. and Peterson, R.G., 1996. An Antarctic circumpolar in surface pressure, wind, temperature and sea-ice extent. Nature, 380: 699–702.

Winograd, I.J., Coplen, T.B., Landwehr, J.M., Riggs, A.C., Ludwig, K.R., Szabo, B.J., Kolesar, P.T. and Revesz, K.M., 1992. Continuous 500,000-year climate record from vein calcite in Devils Hole, Nevada. Science, 258: 255–260.

Wiscombe, W.J. and Warren, S.G., 1980. A model for the spectral albedo of snow. I: pure snow. J. Atmos. Sci., 37: 2712–2733.

Young, M.A. and Bradley, R.S., 1984. Insolation gradients and the paleoclimatic record. In: A.L. Berger, J. Imbrie, J. Hays, G. Kulcha and B. Saltzman (Editors), Milankovitch and Climate. Kluwer, Dordrecht, pp. 707–713.

Zanakis, S.H. and Rustagi, J.S., 1982. Introduction to contributions in regression and correlations. TIMS Studies Manage. Sci., 19: 11–29.

Zielinski, G.A., Mayewski, P.A., Meeker, L.D., Whitlow, S. and Twickler, M.S. 1996. A 110,000-yr record of explosive volcanism from the GISP2 (Greenland) ice core. Quat. Res., 45: 109–118.